1521-009X/42/1/23–27$25.00
Drug Metabolism and Disposition

http://dx.doi.org/10.1124/dmd.113.054429
Drug Metab Dispos 42:23–27, January 2014

Short Communication

Essential Role of the Cytochrome P450 Enzyme CYP2A5 in Olfactory Mucosal Toxicity of Naphthalene[S]

Received August 22, 2013; accepted October 2, 2013

ABSTRACT

Naphthalene (NA), a ubiquitous environmental pollutant that can cause pulmonary and nasal toxicity in laboratory animals, requires cytochrome P450 (P450)–mediated metabolic activation to cause toxicity. Our recent study using a *Cyp2f2*-null mouse showed that CYP2F2 plays an essential role in NA-induced lung toxicity, but not in NA-induced nasal toxicity. The aim of this study was to determine whether mouse CYP2A5, abundantly expressed in nasal olfactory mucosa (OM) and the liver, but less in the lung, plays a major role in the bioactivation and toxicity of NA in the OM. We found, by comparing *Cyp2a5*-null and wild-type (WT) mice, that the loss of CYP2A5 expression led to substantial decreases in rates of NA metabolic activation by OM microsomes. The loss of CYP2A5 did not cause changes in systemic clearance of NA (at 200 mg/kg, i.p.). However, the *Cyp2a5*-null mice were much more resistant than were WT mice to NA-induced nasal toxicity (although not lung toxicity), when examined at 24 hours after NA dosing (at 200 mg/kg, i.p.), or to NA-induced depletion of total nonprotein sulfhydryl in the OM (although not in the lung), examined at 2 hours after dosing. Thus, mouse CYP2A5 plays an essential role in the bioactivation and toxicity of NA in the OM, but not in the lung. Our findings further illustrate the tissue-specific nature of the role of individual P450 enzymes in xenobiotic toxicity, and provide the basis for a more reliable assessment of the potential risks of NA nasal toxicity in humans.

Introduction

Naphthalene (NA), a component of coal tar, crude oil, and cigarette smoke, and a chemical intermediate for the manufacturing of numerous commercial products, is a ubiquitous environmental pollutant (Riviere et al., 1999; McDougal et al., 2000; Preuss et al., 2003). NA exposure can cause tissue-specific toxicity in Clara cells of mouse lung and in epithelial cells of the nasal olfactory mucosa (OM) of rats and mice (Plopper et al., 1992). NA is carcinogenic in both rats and mice (Abdo et al., 2001), and it has been classified as a potential human carcinogen by the International Agency for Research on Cancer (IARC Working Group on the Evaluation of Carcinogenic Risks to Humans, 2002). The mechanism of NA's carcinogenicity is believed to involve repeated cycles of epithelial injury and repair, in connection with NA bioactivation and the resulting acute cytotoxicity (Brusick, 2008).

The bioactivation of NA is mainly catalyzed by cytochrome P450 (P450) enzymes, which produce reactive NA-1,2-epoxide. The epoxide can conjugate with reduced glutathione (GSH), form adducts with sulfhydryl groups in cellular proteins, or be further converted to reactive quinones, diepoxides, and diol epoxides (Buckpitt et al., 2002). Rapid formation of NA oxide and quinones can lead to GSH depletion, increased cellular oxidative stress, and eventually cell death. The high abundance of CYP2F2, a highly active and efficient NA oxidase, in the Clara cells of mouse lung has been proposed to explain the high sensitivity of these cells to NA's cytotoxicity (Buckpitt et al., 1995). The latter hypothesis was confirmed recently by the finding that *Cyp2f2*-null mice are resistant to NA's lung toxicity (Li et al., 2011). However, although CYP2F2 is also expressed in the OM, *Cyp2f2*-null mice were not protected against NA's toxicity in the OM, a result suggesting a more prominent role of other P450 enzymes expressed in the OM (Li et al., 2011).

The aim of this study was to test the hypothesis that CYP2A5, an abundant P450 enzyme expressed in mouse OM (Gu et al., 1998), plays an important role in NA toxicity in the OM. CYP2A5 is active toward numerous drugs and other xenobiotic compounds (Su and Ding, 2004; Wong et al., 2005; Raunio et al., 2008), including many nasal toxicants, such as the herbicide dichlobenil (Xie et al., 2010) and the antithyroid drug methimazole (Xie et al., 2011). Previous studies using recombinant P450 enzymes have shown that human CYP2A6 and CYP2A13, orthologs of mouse CYP2A5, are both active in NA bioactivation (Cho et al., 2006; Fukami et al., 2008); however, evidence for a role of CYP2A5 in mediating the toxicity of NA has yet to be obtained. To test our hypothesis, we compared NA metabolism and toxicity in *Cyp2a5*-null mice, with germline deletion of the *Cyp2a5* gene (Zhou et al., 2010), and wild-type (WT) mice. The *Cyp2a5*-null mouse model has been used in previous studies to demonstrate roles of CYP2A5 in the bioactivation of, and/or tissue toxicity induced by, several other compounds, including dichlobenil (Xie et al., 2010, 2013), acetaminophen (Zhou et al., 2011), methimazole (Xie et al., 2011), 3-methylindole (Zhou et al., 2012a), and the tobacco-specific lung carcinogen 4-(methylnitrosamino)-1-(3-pyridyl)-1-butanone (Zhou et al., 2012b).

This study was supported in part by the National Institutes of Health National Institute of Environmental Health Sciences [Grants ES007462 and ES020867].
dx.doi.org/10.1124/dmd.113.054429.
[S]This article has supplemental material available at dmd.aspetjournals.org.

ABBREVIATIONS: AP-GSH, acetaminophen-glutathione; GSH, reduced glutathione; NA, naphthalene; NA-GSH, naphthalene-glutathione; NPSH, nonprotein sulfhydryl; OM, nasal olfactory mucosa; P450, cytochrome P450; $t_{1/2}$, elimination half-time; T_{max}, time when C_{max} is reached; WT, wild type.

Here, the *Cyp2a5*-null and WT mice, both with a C57BL/6 genetic background, were treated with NA at a dose established in previous studies to induce respiratory tract toxicity in WT mice. The extent of NA-induced OM and lung toxicity was assessed by histological analysis, and through measurements of tissue levels of nonprotein sulfhydryl (NPSH). The impacts of the loss of CYP2A5 expression on microsomal rates of NA metabolic activation in vitro, and on the kinetics of NA clearance in vivo, were also examined. Our results provide definitive evidence that CYP2A5 plays a critical role in mediating NA toxicity in the mouse OM.

Materials and Methods

Chemicals and Animal Treatments. Sources of NA (99% pure), NA-d_8 (99% pure), corn oil (highly refined, low acidity), GSH, NADPH, acetaminophen-glutathione (AP-GSH), naphthalene-glutathione (NA-GSH) standard (consisting of a mixture of all four stereoisomers), and all solvents (dichloromethane, formic acid, methanol, and water, all analytical grade) were the same as described recently (Li et al., 2011). Procedures involving animals were approved by the Institutional Animal Care and Use Committee of the Wadsworth Center (Albany, NY). *Cyp2a5*-null and WT mice were obtained from breeding stocks maintained at the Wadsworth Center. Two- to 3-month old, male mice were treated with a single dose of NA (200 mg/kg, i.p.) in corn oil. Control mice were injected with the vehicle only. Blood samples were collected from the tail at various times after dosing (15 minutes to 24 hours) for preparation of plasma. At 24 hours after NA injection, the mice were euthanized by CO_2 overdose, and noses, lungs, and livers were dissected for histopathological examination. For determination of tissue levels of NA-GSH and NPSH, the liver, lung, and OM were dissected at 2 hours following NA injection. Plasma and tissue samples were stored at −80°C until use.

Determination of Catalytic Activity In Vitro. Microsomal NA metabolism was assayed as described recently (Li et al., 2011), by measuring rates of formation of NA-GSH (Shultz et al., 1999). Reaction mixtures contained 50 mM phosphate buffer (pH 7.4), 2.5∼200 μM NA (added in 2 μl of methanol), 10 mM GSH, 0.2 mg/ml (for lung) or 0.05 mg/ml (for OM) microsomal protein, and 1 mM NADPH, in a final volume of 0.2 ml. The reaction was carried out at 37°C for 5 minutes. AP-GSH was added as the internal standard. NA-GSH was determined using liquid chromatography–tandem mass spectrometry (Li et al., 2011). For controls, the reaction was terminated prior to NADPH addition. Apparent K_m and V_{max} values for OM microsomal formation of NA-GSH were estimated by nonlinear regression to a Michaelis-Menten equation and the data reported as the mean ± S.D. of values determined for three separate microsomal samples, each prepared from tissues pooled from five mice.

Determination of NA, NA-GSH, and NPSH. Plasma NA levels were determined using gas chromatography–mass spectrometry, as described (Li et al., 2011), with NA-d_8 as an internal standard. All procedures were carried out in sealed tubes to prevent NA evaporation. Calibration curves were constructed using authentic NA (0.02–20 μg/ml) added to blank mouse plasma. NA-GSH levels in plasma and tissue homogenate samples from individual mice were determined as described (Li et al., 2011), using liquid chromatography–tandem mass spectrometry, with AP-GSH as an internal standard. Calibration curves were constructed using authentic NA-GSH (0.05–10 μg/ml) added to blank mouse plasma.

NPSH was determined as described (Xie et al., 2010), using an established method (Tonge et al., 1998). Liver and lung tissues were homogenized with a Polytron homogenizer (model GT 10-35; Kinematica, Bohemia, NY), whereas OM from individual mice was homogenized using a Bullet Blender (Next Advance, Averill Park, NY) (Xie et al., 2010). Reduced glutathione was used as the standard.

Histopathological Examination. Liver and lung tissues were fixed in 10% neutral buffered formalin, whereas the nose was fixed in Bouin's solution. Paraffin sections (4 μm) were stained with hematoxylin and eosin, for histopathological analysis (Gu et al., 2003, 2005). Nose tissue blocks were prepared according to Young (1981). The severity of lesions in the OM was graded, as described (Gu et al., 2005). Tissue sectioning and staining were performed at the Wadsworth Center Pathology Core Facility. Images were obtained using a Nikon model 50i light microscope (Nikon, Tokyo, Japan), fitted with a digital camera, at the Wadsworth Center Light Microscopy Core.

Other Methods. Lung and OM microsomes were prepared as described previously (Gu et al., 1997). Pharmacokinetic parameters were calculated by noncompartmental pharmacokinetic analysis using the WinNonlin software (Pharsight, Mountain View, CA). Enzyme kinetic parameters were calculated using Prism (GraphPad Software, San Diego, CA). The statistical significance of differences between two groups in various parameters was examined using Student's *t* test.

Results and Discussion

Role of CYP2A5 in OM Microsomal NA Metabolic Activation In Vitro. The rates of NA-GSH formation in incubations of NA with OM or lung microsomes were compared between *Cyp2a5*-null and WT mice, with NA at 100 μM. OM rates were significantly higher in WT mice (0.62 ± 0.04 nmol/min/mg protein, mean ± S.D.; $n = 3$) than in *Cyp2a5*-null mice (0.38 ± 0.01 nmol/min/mg protein; $n = 3$), whereas lung rates were similar between the two strains (1.0 ± 0.1 and 1.1 ± 0.1 nmol/min/mg protein, respectively, for WT and *Cyp2a5*-null mice; $n = 3$). OM microsomal activity was then further analyzed for determination of apparent kinetic constants. As shown in Fig. 1, OM rates were consistently higher in WT than in *Cyp2a5*-null mice, over a broad range of NA concentrations. The apparent V_{max} value was significantly higher in WT mice (0.74 ± 0.01 nmol/min/mg protein, mean ± S.D.; $n = 3$) than in the null mice (0.41 ± 0.01 nmol/min/mg protein; $P < 0.01$ compared with WT), whereas the apparent K_m values were only slightly greater in WT mice (13.7 ± 1.0 μM) than in the *Cyp2a5*-null mice (11.0 ± 1.1 μM; $P < 0.05$). The apparent catalytic efficiency (V_{max}/K_m; ml/min/mg protein) was 0.054 in WT OM and 0.037 in *Cyp2a5*-null OM. Thus, CYP2A5 plays an important role in NA bioactivation in the OM, and it seems to have (∼50%) greater catalytic efficiency toward NA than the other P450 enzymes in OM microsomes.

Role of CYP2A5 in NA Metabolism In Vivo. The loss of CYP2A5 in the *Cyp2a5*-null mice did not impact systemic elimination of NA or its major GSH-trapped metabolite NA-GSH. The pharmacokinetic profiles of plasma NA or NA-GSH were similar between WT and *Cyp2a5*-null mice treated with NA at 200 mg/kg (i.p.) (Supplemental Fig. 1; Table 1). Although the *Cyp2a5*-null mice had slightly lower T_{max} values for plasma NA than WT mice had, there

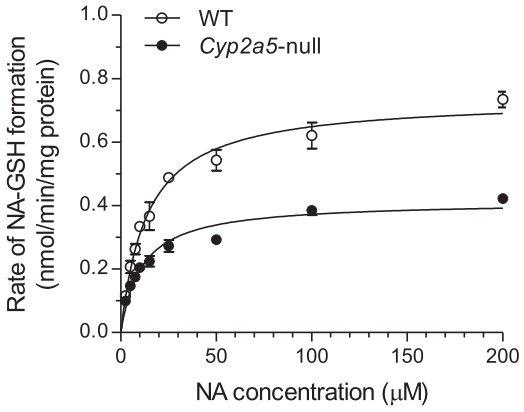

Fig. 1. Substrate-velocity curves for in vitro NA-GSH formation in OM microsomes. Contents of reaction mixtures are described in *Materials and Methods*. Microsomes were prepared from pooled OM from five 2- to 3-month-old male mice. The rates of NA-GSH formation were determined at various NA concentrations (2.5–200 μM). The data (means ± S.D., $n = 3$) were curve-fitted to the Michaelis-Menten equation.

TABLE 1

Pharmacokinetic parameters for plasma NA and NA-GSH in mice treated with NA at 200 mg/kg

Two- to 3-month-old male WT and *Cyp2a5*-null mice were treated intraperitoneally with NA (at 200 mg/kg). Tail blood samples were collected from individual mice at various time points after dosing, for determination of plasma concentrations of NA and NA-GSH, which were used to calculate pharmacokinetic parameters. Values represent means ± S.D. (n = 5–6 for each strain). The plasma concentration-time curves are shown in Supplemental Fig. 1.

Analyte and Strain	$t_{1/2}$	T_{max}	C_{max}	$AUC_{0\text{-}8h}$	CL/F
	h	*h*	*μg/ml*	*μg*h/ml*	*ml/h*
NA					
WT	1.0 ± 0.4	0.5 ± 0.1	2.2 ± 0.3	5.0 ± 1.6	940 ± 290
Cyp2a5-null	0.8 ± 0.1	0.3 ± 0.1[a]	2.7 ± 0.2	5.8 ± 1.6	800 ± 210
NA-GSH					
WT	0.8 ± 0.3	2.0 ± 0	4.4 ± 0.8	12.6 ± 3.3	N/A
Cyp2a5-null	0.7 ± 0.1	1.4 ± 0.8	3.9 ± 1.5	10.6 ± 4.1	N/A

$AUC_{0\text{-}8h}$, area under the concentration-time (0-8h) curve; CL, clearance; F, bioavailability; CL/F, total body clearance instead of CL, given that F is not known; N/A, not applicable.
[a] $P < 0.01$, Student's t test, compared with corresponding WT values.

was no significant difference in $t_{1/2}$, C_{max}, area under the concentration-time curve, or CL/F values for either NA or NA-GSH. Thus, the loss of CYP2A5 expression did not alter systemic clearance of NA administered intraperitoneally.

Tissue levels of NA-GSH were also determined, in the OM, lung, and liver, at 2 hours after the NA treatment to determine the role of CYP2A5 in local NA metabolic activation in vivo. As shown in Table 2, the loss of CYP2A5 was associated with a 50% decrease in NA-GSH levels (compared with WT mice) in the OM, but had no effects on liver and lung NA-GSH levels. This result indicated that CYP2A5 plays a major role in NA metabolic activation in the OM, but not in the liver or lung.

Role of CYP2A5 in NA-Induced Nasal Toxicity. NA is known to cause injury to the lung and OM regardless of the route of administration (Buckpitt et al., 2002). To determine whether CYP2A5 plays any role in NA toxicity, we compared the extent of tissue injury in WT and *Cyp2a5*-null mice treated with a known toxic NA dose (200 mg/kg, i.p.; Plopper et al., 1992) at 24 hours after dosing (Fig. 2). Obvious pathological changes were observed in NA-treated WT mice, in both the olfactory epithelium and submucosa, especially in the nasal septum. Cells of the submucosal glands displayed features of coagulative necrosis and nuclear disintegration. The lesions in the epithelium included deformation and detachment. Remarkably, no lesion was observed in any of the NA-treated *Cyp2a5*-null mice examined. This result strongly supports the hypothesis that CYP2A5 plays a critical role in mediating the cytotoxicity of NA in the OM.

Signs of tissue damage, including necrosis and detachment of both Clara cells and ciliated airway epithelial cells, were also detected in the lungs of NA-treated mice (Fig. 2). However, in contrast to the situation for OM, and consistent with the absence of a significant impact of CYP2A5 loss on lung microsomal activity toward NA, there was no noticeable difference in the severity of lung toxicity between the *Cyp2a5*-null and WT mice. No obvious hepatotoxicity was observed in either WT or *Cyp2a5*-null mice at the dose studied (data not shown).

Levels of tissue NPSH, a marker of reactive metabolite formation in vivo (Phimister et al., 2004), were also determined for WT and *Cyp2a5*-null mice at 2 hours after NA dosing at 200 mg/kg (Table 2). For the liver, NPSH levels decreased by ~75% in WT mice and ~51% in *Cyp2a5*-null mice after the NA treatment, compared with corresponding vehicle-treated mice, a result indicating a relatively minor role of CYP2A5 in hepatic NA metabolic activation. Notably, the residual hepatic NPSH levels were still high in NA-treated mice, presumably explaining the absence of hepatotoxicity. For the lung, NPSH levels decreased by ~40% in both mouse strains after the NA treatment, consistent with the histopathological data showing that CYP2A5 does not play a significant role in NA-induced pneumotoxicity. For the OM, NPSH levels decreased by ~94% in WT mice, but only ~44% in *Cyp2a5*-null mice, after the NA treatment, compared with corresponding vehicle-treated mice. The residual NPSH levels in the OM were ~10 times greater in NA-treated *Cyp2a5*-null mice, compared with NA-treated WT mice, consistent with the absence of nasal tissue injury in this group at 24 hours after NA treatment.

Respective Roles of CYP2A5 and CYP2F2 in NA-Induced Respiratory Toxicity. The difference between tissues concerning the impact of CYP2A5 loss on NA-induced toxicity was consistent with in vitro metabolic data, which showed an obvious decrease in rates of microsomal NA bioactivation in OM, but little change in the lung. Similarly, the tissue difference in NA toxicity was consistent with in vivo biomarker data, which showed that the levels of NA-GSH, a marker for reactive NA metabolites produced in vivo, were significantly decreased only in OM, but not in the lung or liver. On the contrary, rates of NA clearance were similar between the *Cyp2a5*-null mouse and the WT mouse, a fact indicating that the strain difference in OM toxicity did not result from a change in NA bioavailability in the *Cyp2a5*-null mice. The latter data also indicated that CYP2A5 did not make a notable contribution to circulating levels of NA-GSH, at least at the dose examined; this is consistent with our earlier data from *Cyp2f2*-null mice that CYP2F2 plays a predominant role in the systemic clearance of NA (Li et al., 2011).

TABLE 2

Tissue levels of NA-GSH and NPSH in WT and *Cyp2a5*-null mice

Two- to 3-month-old male WT and *Cyp2a5*-null mice were given a single intraperitoneal injection of either vehicle alone or NA at 200 mg/kg. Tissues were collected from individual mice at 2 hours after dosing. The data represent means ± S.D. (n = 3–6). The numbers in parentheses indicate null/WT (percentage).

Tissue	Strain	NA-GSH	NPSH		
			Vehicle-Treated	NA-Treated	NA-Induced Decrease
		μg/g tissue	*μmol/g tissue*	*μmol/g tissue*	*%*
Liver	WT	53.6 ± 7.2	8.4 ± 3.1	2.1 ± 0.1[a]	75
	Cyp2a5-null	49.8 ± 6.6 (93)	6.7 ± 1.6	3.3 ± 0.7[a]	51
Lung	WT	5.4 ± 1.4	1.2 ± 0.2	0.7 ± 0.1[a]	42
	Cyp2a5-null	4.5 ± 1.1 (83)	1.4 ± 0.3	0.9 ± 0.3[a]	36
OM	WT	1.8 ± 0.4	1.8 ± 0.1	0.1 ± 0.1[a]	94
	Cyp2a5-null	0.9 ± 0.5 (50)[b]	1.8 ± 0.1	1.0 ± 0.4[a,b]	44

[a] $P < 0.01$, NA-treated compared with corresponding vehicle control values.
[b] $P < 0.01$, *Cyp2a5*-null compared with corresponding WT values.

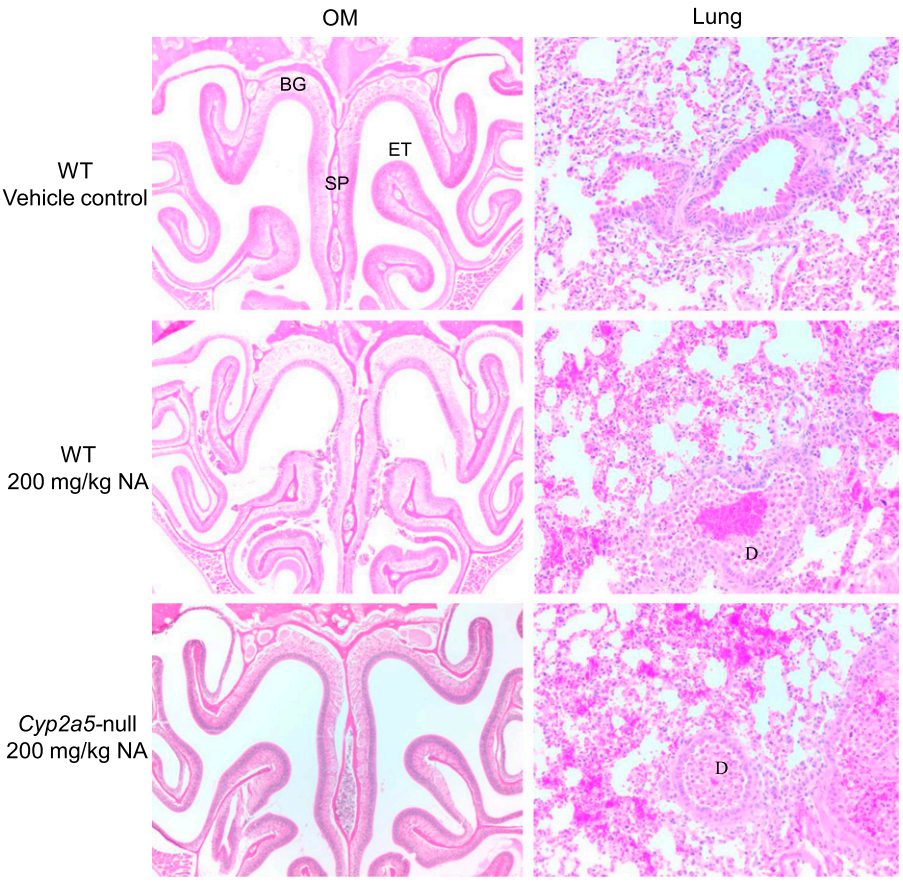

Fig. 2. Histopathological analysis of nasal mucosal injury caused by NA treatment in WT and *Cyp2a5*-null mice. Two- to 3-month-old male mice were treated with a single i.p. injection of NA (at 200 mg/kg), or with the vehicle alone. Tissues were obtained for histopathological examination at 24 hours after treatment. For the nose, representative H&E-stained cross-sections of the nasal cavity (40×), obtained at level 3 (Young, 1981), are shown. Vehicle-treated mice had normal ethmoidal turbinates (ET) and nasal septum (SP) lined by a thick, pseudostratified olfactory neuroepithelium in the dorsomedial part, and a clear nasal passage; NA-treated WT C57BL/6 mice ($n = 6$) showed extensive injury to the OM, evident as epithelial necrosis, detachment, sloughing, and ulceration; NA-treated *Cyp2a5*-null mice ($n = 5$) showed essentially normal olfactory epithelium and Bowman's glands (BG). For the lung, representative H&E-stained sections (40×) are shown. Control mice had a normal bronchiolar epithelium; NA-treated WT mice ($n = 6$) and *Cyp2a5*-null mice ($n = 5$) both showed necrosis and detachment of cells from the epithelium, with abundant cell debris (D) present in the airway lumen.

NA was administered intraperitoneally in this and most other studies on mechanisms of NA toxicity. The respective roles of CYP2A5 and CYP2F2 in NA's nasal and lung toxicities will unlikely change for NA exposure through other routes, such as inhalation, given the common location of the OM and lung in the respiratory tract. Furthermore, the tissue-selective contributions of the two enzymes to NA toxicity, which are at least partly determined by their relative abundances in the OM and lung, will likely hold true for a broad range of NA doses, even though only a single dose was examined in the present study, as implied from the in vitro activity data for the *Cyp2a5*-null (here) and *Cyp2f2*-null (Li et al., 2011) mice. Notably, a detailed biochemical comparison of the NA metabolism by CYP2A5 and CYP2F2 in a reconstituted system remains to be conducted, to determine the relative catalytic efficiencies of the two enzymes, even though previous microsomal analysis showed that the apparent catalytic efficiencies for NA bioactivation in the lung (catalyzed mainly by CYP2F2) and OM (catalyzed mainly by CYP2A5) of WT mice were comparable (Li et al., 2011).

Summary

For the first time, we showed that mouse CYP2A5 plays an essential role in the bioactivation and toxicity of NA in the OM, but not in the lung. Our findings validate the respective roles of CYP2A5 and CYP2F2 in NA-induced nasal and pulmonary toxicity in mice, and illustrate the complexity of the metabolic mechanisms underlying site-specific toxicity of xenobiotic compounds in the respiratory tract, which dictates the necessity to study toxicant metabolism in each target tissue. These findings also provide a basis for predicting the toxic consequences of NA metabolism by human CYP2A6, CYP2A13, and CYP2F1 in the lung and nasal mucosa of exposed individuals.

Acknowledgments

The authors gratefully acknowledge the services of the Pathology Core and the Advanced Light Microscopy and Image Analysis Core Facilities of the Wadsworth Center. The authors thank Drs. Alan Buckpitt and Dexter Morin of the University of California Davis for providing NA-GSH standards, and Ms. Weizhu Yang for assistance with mouse breeding.

Wadsworth Center, New York State Department of Health, and School of Public Health, State University of New York at Albany, Albany, New York (J.H., L.S., L.L., X.Z., F.X., J.D., X.D.); and Institute of Materia Medica, Chinese Academy of Medical Sciences & Perking Union Medical College, Beijing, China (J.H., L.S., Y.L.)

Jinping Hu
Li Sheng
Lei Li
Xin Zhou
Fang Xie
Jaime D'Agostino
Yan Li
Xinxin Ding

Authorship Contributions

Participated in research design: Hu, Sheng, L. Li, Zhou, Xie, D'Agostino, Y. Li, Ding.

Conducted experiments: Hu, Sheng, L. Li, Zhou, Xie.

Performed data analysis: Hu, Sheng, L. Li, Ding.

Wrote or contributed to the writing of the manuscript: Hu, L. Li, Y. Li, Ding.

References

Abdo KM, Grumbein S, Chou BJ, and Herbert R (2001) Toxicity and carcinogenicity study in F344 rats following 2 years of whole-body exposure to naphthalene vapors. *Inhal Toxicol* **13**: 931–950.

Brusick D (2008) Critical assessment of the genetic toxicity of naphthalene. *Regul Toxicol Pharmacol* **51**(2, Suppl)S37–S42.

Buckpitt A, Boland B, Isbell M, Morin D, Shultz M, Baldwin R, Chan K, Karlsson A, Lin C, and Taff A, et al. (2002) Naphthalene-induced respiratory tract toxicity: metabolic mechanisms of toxicity. *Drug Metab Rev* **34**:791–820.

Buckpitt A, Chang AM, Weir A, Van Winkle L, Duan X, Philpot R, and Plopper C (1995) Relationship of cytochrome P450 activity to Clara cell cytotoxicity. IV. Metabolism of naphthalene and naphthalene oxide in microdissected airways from mice, rats, and hamsters. *Mol Pharmacol* **47**:74–81.

Cho TM, Rose RL, and Hodgson E (2006) In vitro metabolism of naphthalene by human liver microsomal cytochrome P450 enzymes. *Drug Metab Dispos* **34**:176–183.

Fukami T, Katoh M, Yamazaki H, Yokoi T, and Nakajima M (2008) Human cytochrome P450 2A13 efficiently metabolizes chemicals in air pollutants: naphthalene, styrene, and toluene. *Chem Res Toxicol* **21**:720–725.

Gu J, Cui H, Behr M, Zhang L, Zhang QY, Yang W, Hinson JA, and Ding X (2005) In vivo mechanisms of tissue-selective drug toxicity: effects of liver-specific knockout of the NADPH-cytochrome P450 reductase gene on acetaminophen toxicity in kidney, lung, and nasal mucosa. *Mol Pharmacol* **67**:623–630.

Gu J, Walker VE, Lipinskas TW, Walker DM, and Ding X (1997) Intraperitoneal administration of coumarin causes tissue-selective depletion of cytochromes P450 and cytotoxicity in the olfactory mucosa. *Toxicol Appl Pharmacol* **146**:134–143.

Gu J, Weng Y, Zhang QY, Cui H, Behr M, Wu L, Yang W, Zhang L, and Ding X (2003) Liver-specific deletion of the NADPH-cytochrome P450 reductase gene: impact on plasma cholesterol homeostasis and the function and regulation of microsomal cytochrome P450 and heme oxygenase. *J Biol Chem* **278**:25895–25901.

Gu J, Zhang QY, Genter MB, Lipinskas TW, Negishi M, Nebert DW, and Ding X (1998) Purification and characterization of heterologously expressed mouse CYP2A5 and CYP2G1: role in metabolic activation of acetaminophen and 2,6-dichlorobenzonitrile in mouse olfactory mucosal microsomes. *J Pharmacol Exp Ther* **285**:1287–1295.

IARC Working Group on the Evaluation of Carcinogenic Risks to Humans (2002) Some traditional herbal medicines, some mycotoxins, naphthalene and styrene. *IARC Monogr Eval Carcinog Risks Hum* **82**:1–556 IARC, Lyon, France.

Li L, Wei Y, Van Winkle L, Zhang QY, Zhou X, Hu J, Xie F, Kluetzman K, and Ding X (2011) Generation and characterization of a *Cyp2f2*-null mouse and studies on the role of CYP2F2 in naphthalene-induced toxicity in the lung and nasal olfactory mucosa. *J Pharmacol Exp Ther* **339**:62–71.

McDougal JN, Pollard DL, Weisman W, Garrett CM, and Miller TE (2000) Assessment of skin absorption and penetration of JP-8 jet fuel and its components. *Toxicol Sci* **55**:247–255.

Phimister AJ, Lee MG, Morin D, Buckpitt AR, and Plopper CG (2004) Glutathione depletion is a major determinant of inhaled naphthalene respiratory toxicity and naphthalene metabolism in mice. *Toxicol Sci* **82**:268–278.

Plopper CG, Suverkropp C, Morin D, Nishio S, and Buckpitt A (1992) Relationship of cytochrome P-450 activity to Clara cell cytotoxicity. I. Histopathologic comparison of the respiratory tract of mice, rats and hamsters after parenteral administration of naphthalene. *J Pharmacol Exp Ther* **261**:353–363.

Preuss R, Angerer J, and Drexler H (2003) Naphthalene—an environmental and occupational toxicant. *Int Arch Occup Environ Health* **76**:556–576.

Raunio H, Hakkola J, and Pelkonen O2008. The CYP2A subfamily, in *Cytochrome P450 Role in Metabolism and Toxicity of Drugs and Other Xenobiotics* (Ioannides C ed) pp 151–171, Advancing the Chemical Sciences Publishing, Cambridge, UK.

Riviere JE, Brooks JD, Monteiro-Riviere NA, Budsaba K, and Smith CE (1999) Dermal absorption and distribution of topically dosed jet fuels jet-A, JP-8, and JP-8(100). *Toxicol Appl Pharmacol* **160**:60–75.

Shultz MA, Choudary PV, and Buckpitt AR (1999) Role of murine cytochrome P-450 2F2 in metabolic activation of naphthalene and metabolism of other xenobiotics. *J Pharmacol Exp Ther* **290**:281–288.

Su T and Ding X (2004) Regulation of the cytochrome P450 2A genes. *Toxicol Appl Pharmacol* **199**:285–294.

Tonge RP, Kelly EJ, Bruschi SA, Kalhorn T, Eaton DL, Nebert DW, and Nelson SD (1998) Role of CYP1A2 in the hepatotoxicity of acetaminophen: investigations using Cyp1a2 null mice. *Toxicol Appl Pharmacol* **153**:102–108.

Wong HL, Murphy SE, and Hecht SS (2005) Cytochrome P450 2A-catalyzed metabolic activation of structurally similar carcinogenic nitrosamines: N'-nitrosonornicotine enantiomers, N-nitrosopiperidine, and N-nitrosopyrrolidine. *Chem Res Toxicol* **18**:61–69.

Xie F, D'Agostino J, Zhou X, and Ding X (2013) Bioactivation of the nasal toxicant 2,6-dichlorobenzonitrile: an assessment of metabolic activity in human nasal mucosa and identification of indicators of exposure and potential toxicity. *Chem Res Toxicol* **26**:388–398.

Xie F, Zhou X, Behr M, Fang C, Horii Y, Gu J, Kannan K, and Ding X (2010) Mechanisms of olfactory toxicity of the herbicide 2,6-dichlorobenzonitrile: essential roles of CYP2A5 and target-tissue metabolic activation. *Toxicol Appl Pharmacol* **249**:101–106.

Xie F, Zhou X, Genter MB, Behr M, Gu J, and Ding X (2011) The tissue-specific toxicity of methimazole in the mouse olfactory mucosa is partly mediated through target-tissue metabolic activation by CYP2A5. *Drug Metab Dispos* **39**:947–951.

Young JT (1981) Histopathologic examination of the rat nasal cavity. *Fundam Appl Toxicol* **1**: 309–312.

Zhou X, D'Agostino J, Li L, Moore CD, Yost GS, and Ding X (2012a) Respective roles of CYP2A5 and CYP2F2 in the bioactivation of 3-methylindole in mouse olfactory mucosa and lung: studies using Cyp2a5-null and Cyp2f2-null mouse models. *Drug Metab Dispos* **40**:642–647.

Zhou X, D'Agostino J, Xie F, and Ding X (2012b) Role of CYP2A5 in the bioactivation of the lung carcinogen 4-(methylnitrosamino)-1-(3-pyridyl)-1-butanone in mice. *J Pharmacol Exp Ther* **341**:233–241.

Zhou X, Wei Y, Xie F, Laukaitis CM, Karn RC, Kluetzman K, Gu J, Zhang QY, Roberts DW, and Ding X (2011) A novel defensive mechanism against acetaminophen toxicity in the mouse lateral nasal gland: role of CYP2A5-mediated regulation of testosterone homeostasis and salivary androgen-binding protein expression. *Mol Pharmacol* **79**:710–723.

Zhou X, Zhuo X, Xie F, Kluetzman K, Shu YZ, Humphreys WG, and Ding X (2010) Role of CYP2A5 in the clearance of nicotine and cotinine: insights from studies on a *Cyp2a5*-null mouse model. *J Pharmacol Exp Ther* **332**:578–587.

Address correspondence to: Dr. Xinxin Ding, Wadsworth Center, New York State Department of Health, Empire State Plaza, Box 509, Albany, NY 12201-0509. E-mail: xding@wadsworth.org